Resilient Model based Predictive Control Scheme Inspired by Artificial Intelligence Methods for Grid-Interactive Inverters

Matthew Baker, *Student Member*, *IEEE,* Hassan Althuwaini, *Student Member*, *IEEE,* and Mohammad B. Shadmand, *Senior Member, IEEE*

Intelligent Power Electronics at Grid Edge (IPEG) Research Laboratory
Department of Electrical and Computer Engineering, University of Illinois Chicago
mbaker36@uic.edu; halthu2@uic.edu, shadmand@uic.edu

***Abstract* — This paper presents an intelligent predictive control schemes that integrates model and data-driven schemes for enhancing the resiliency of grid-interactive inverters to mitigate the impact of dynamic grid condition on model-based control performance. Conventional model predictive control (MPC) techniques feature several advantages such as fast dynamic response, single loop optimization instead of cascaded control schemes, and several others that are enabled by enhancements in micro-controllers for control of power electronics converters. These inherent features of MPC enable design of control schemes with advance functionalities for grid-interactive inverters. MPC efficacy is highly dependent on prediction accuracy of control variables. The prediction accuracy for a predictive controlled grid-interactive inverter depends on many factors including the controller knowledge on filter model parameters and variation of grid impedance. The variation of grid impedance can impact the current prediction accuracy due to the effect of the equivalent impedance on the effective impedance the inverter experiences at its point of common coupling (PCC). The grid impedance variation is expected in future power electronics dominated grid (PEDG) with multiple point of common coupling (MPCC). The proposed resilient artificial intelligence (AI) inspired MPC scheme addresses these challenges towards improving the performance of grid-interactive inverters in PEDG. This is done through the introduction of a Learned Impedance Factor to the MPC cost formulation equation. In this paper an overview of the proposed integrated data-driven and model-based control scheme is provided, and results demonstrate the proposed controller improves the THD and tracking error compared to conventional MPC that is purely model-based.**

***Keywords* – neural network, model predictive control, power electronics dominated grid, self-learning inverter, smart inverter, grid-interactive inverter**

I. Introduction

Model predictive control (MPC) is a promising control scheme for power converters which uses a model of a power converter to select optimal switching states [1-3]. MPC is capable of delivering a multitude of control objectives with a simple model of the power electronics system [4, 5]. By creating a model based cost optimization function, MPC is able to determine optimal switching states at every sampling instant [6-8]. The benefits of MPC for power electronics is enhanced with Finite Set MPC (FS-MPC) using finite number of switching states for online optimization. The smaller set of possible solutions leads to simplifying the optimization problem and reducing the computational effort [9-11]. For proper operation and prediction of control variables, MPC requires accurate values of system parameters, such as filter inductors and capacitors. Additionally, other disturbances such as changes in grid impedance will lead to inaccurate prediction of control variables, such as injected current, in a grid-interactive inverter. These kinds of disturbances are expected in future power electronics dominated grids (PEDG) [6, 12, 13] which impacts the MPC efficacy and limits the grid-interaction of inverters. The futuristic PEDG features interconnected grid clusters with multiple point of common coupling (MPCC) which can create variation in grid characteristics and consequently the control performance of power electronic based generations. MPC can provide utility for realizing grid-interactive inverters, which motivates numerous researchers in academia and industry to investigate this tool's capabilities. This is evident by the uptick number of published articles in literature on model predictive controlled inverters [14], [15].

This paper addresses one of the challenges for implementation of MPC for grid-interactive inverters under uncertainty in model parameters and grid condition. These uncertainties lead to higher error in tracking control variables and when propagated among several inverters in a grid cluster, which could occur with high penetration of power electronics source, could jeopardize the PEDG stability [6], [16]. Several methos proposed in literature to mitigate the parameters disturbance in MPC for power converters, for instance [17] used simplified repetitive control, [18] creates a predictive controller based on parameter estimation instead of a model, and [19] utilized an auto-tuned algorithm to finely adjust the model parameters. To the best of the author's knowledge, none of these works and others published in literature are discussing the impact of grid impedance variation on prediction accuracy of control variable in a grid-interactive inverter. Weak grid conditions are observable when the short circuit ratio of the grid reveals high impedance as seen at PCC [20]. The literature has provided adaptive solutions to accounting for weak grid

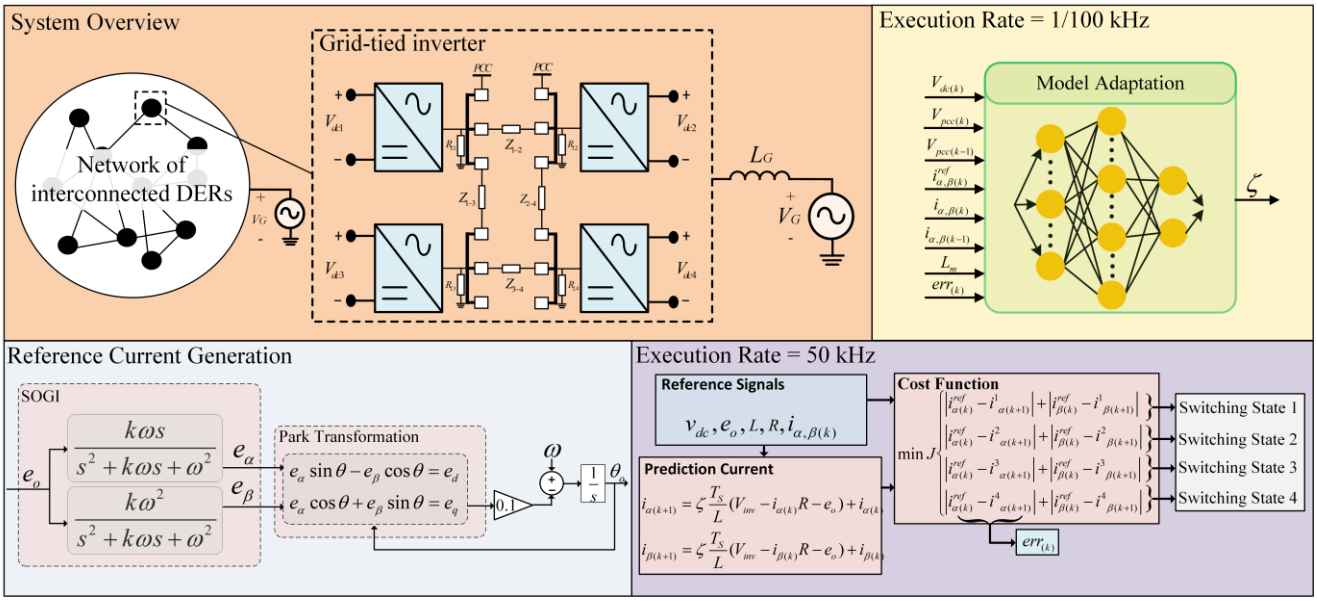

Fig. 1. Proposed AI inspired MPC for grid-interactive inverters with disturbance mitigation capability. The proposed controller incorporates a Learned Impedance Factor "ζ" into the MPC cost function subject to minimization.

conditions: A virtual impedance is used in [21] to shape the grid and thus improve the SCR to create a stiff grid, [22, 23] both utilize the impedance shaping to dampen unstable grids, and [24] adjusts the MPC objective during weak grid conditions to prevent resonance which causes instability. However, while these techniques can maintain grid stability, they lack the ability to adapt to uniformly react to all disturbance sources which affect the converter impedance in a general fashion. Thus, there is a need to realize a method for MPC to mitigate the impact of any grid impedance variation on the control performance while leveraging the inherent features of MPC for efficient grid-interaction of inverters.

This paper proposes an integrated data-driven and model-based approach to realize a resilient predictive control scheme for grid-interactive inverters that mitigates the impact of potential disturbances in the network impedance. This is accomplished through a neural network approach which implements a 'Learned Impedance Factor' into the model during state optimization. The proposed learning approach objective is to determine the effective impedance that the inverter bridge experiences at its terminals instead of the rated filter parameters from manufacturer. In fact, the proposed approach is optimizing the model in real-time by taking into account the variation in grid-impedance. The learning approach is based on tracking error of the controller which introduced in the MPC framework as a learned impedance factor.

The remainder of the paper is as follows: Section II covers the system modeling for the MPC, Section III covers the artificial intelligence (AI) disturbance adaptation and the neural network training, Section IV covers the case study used to verify the operation of the proposed technique, and Section V concludes the paper and summarizes the results.

II. System Modeling

The general structure of the proposed MPC-based controller is depicted in Fig. 1. The dc source represents a battery storge unit and the inverter is interfaced to the grid via an L filter. A phase locked loop (PLL) with a second order generalized integrator (SOGI)-based orthogonal signal generator (OSG) is utilized to detect the grid voltage angle and split the reference to the $\alpha\beta$-framework. The inherent filtering capabilities of the SOGI OSG and moving to the αβ-framework make the reference voltage and current more resistant for any distortion and irregularity on grid conditions [25]. The reference of the decoupled active and reactive power is constructed on the dq framework and is given by,

$$P_{(k)} = \frac{1}{2} e_{d(k)} i_{d(k)} + \frac{1}{2} e_{q(k)} i_{q(k)}$$
$$Q_{(k)} = \frac{1}{2} e_{q(k)} i_{d(k)} - \frac{1}{2} e_{d(k)} i_{q(k)} \quad (1)$$

where P_k and Q_k are active and reactive power. $e_{d,k}$ and $e_{q,k}$ are the grid voltage in the dq rotating frame, $i_{d,k}$ and $i_{q.k}$ are decoupled current in the rotating frame. Rearranging equation (1) yields the current reference, which is given in (2).

$$i_{d(k)} = \frac{2(P_{(k)} e_{d(k)} + Q_{(k)} e_{q(k)})}{{e_{d(k)}}^2 + {e_{q(k)}}^2}$$
$$i_{q(k)} = \frac{2(P_{(k)} e_{q(k)} - Q_{(k)} e_{d(k)})}{{e_{d(k)}}^2 + {e_{q(k)}}^2} \quad (2)$$

The inverse Park transformation is used to convert the reference current components from the rotating frame to the stationary reference frame from (2),

$$i_{\alpha,\beta(k)} = i_{d(k)} \sin(\theta_{(k)}) + i_{q(k)} \cos(\theta_{(k)}) \quad (3)$$

where θ_k denotes the grid angle detected by the PLL. At the PCC with the grid, the filter dynamic equation is given by,

$$\frac{di}{dt} = \frac{1}{L}(V_{inv} - ri - e_o) \tag{4}$$

where L is the inductance of the filter, and r is the equivalent series resistance. The Euler forward method is used to discretize (4) in order to predict the current one step ahead in horizon of time:

$$i_{\alpha(k+1)} = \zeta \frac{T_S}{L}(V_{inv} - i_{\alpha(k)} r - e_o) + i_{\alpha(k)} \tag{5a}$$

$$i_{\beta(k+1)} = \zeta \frac{T_S}{L}(V_{inv} - i_{\beta(k)} r - e_o) + i_{\beta(k)} \tag{5b}$$

The inverter output current is estimated by (5a) and (5b) for the next sampling interval, (k+1), where the corresponding voltage, e_o, is calculated from the feasible switching states. The learned impedance factor, ζ, adapts the predicted current in response to any impedance disturbances. The process of creating and adjusting ζ is covered in Section III. The orthogonal grid voltage and current signal is created via SOGI module, the transfer function is given by,

$$\frac{x_\alpha(s)}{x(s)} = \frac{k\omega s}{s^2 + k\omega s + \omega^2}$$
$$\frac{x_\beta(s)}{x(s)} = \frac{k\omega^2}{s^2 + k\omega s + \omega^2} \tag{6}$$

where k is the SOGI gain and ω is the fundamental angular frequency. A cost function which minimizes the error is then derived as follow:

$$J = \left|i_{\alpha(k)} - i_{\alpha(k+1)}\right| + \left|i_{\beta(k)} - i_{\beta(k+1)}\right| \tag{7}$$

III. Artifical Intelligence Disturbance Detection

A. Learned Impedance Factor

The conventional MPC approach is appropriate for controlling the inverter, provided the model accurately depicts the physical system. However, without any method of responding to grid disturbances, the MPC can become unstable or unsuitable for grid connection according to grid standards. Thus, to improve the robustness of the MPC, the "Learned Impedance Factor" ζ is introduced to the MPC in (5a) and (5b) to improve the performance of the controller and account for any disturbance which affect the system impedance.

TABLE. I: Neural Network Training Parameters

Parameter	Value
DC Link Voltage	400 V
Grid Voltage	120 V_{RMS}
Sampling frequency	20 kHz
Grid Frequency	60 Hz
R_f	0.05 Ω
P_{ref}	3 kW
L_f	2 mH
L_g	0.5: 5.0 mH
L_{error}	50 : 150 %

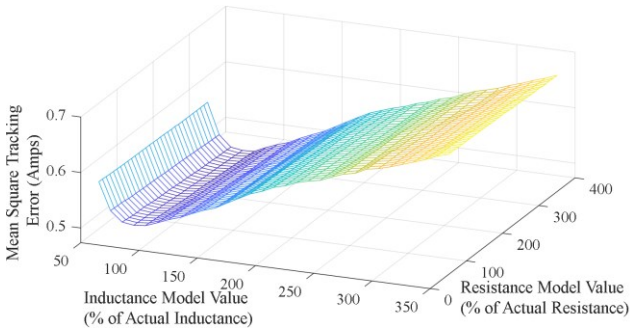

Fig. 2. Impact of Inductance and Resistance disturbance in Tracking Error

Disturbances to the conventional MPC scheme can be introduced by change in grid condition and transitioning from stiff grid to weak grid and ultra-weak grid. The grid strength of Fig. 1 can be determined by the short circuit ratio (SCR)

$$SCR = \frac{V_g^2 / L_g(2\pi f)}{P_{ref}} \tag{8}$$

Where V_g is the RMS of the grid voltage, L_g is the grid impedance, f is the grid frequency, and P_{ref} is the active power reference. The grid is stiff when SCR > 10, weak when 3 ≤ SCR ≤ 10, and ultra-weak when SCR < 3 [26]. From this, the design principle for determining ζ is to adapt predictions of control objectives, i.e. the inverter output current, to changes in L_g during grid condition variation.

B. Neural Network Data Collection

A neural network approach is used for determining ζ in this paper. Network configuration begins with the collection of training and testing data. For data collection, it is desired to reduce the total amount of variables which affect the system to minimize training time and network complexity. As the goal of the network is to reduce the cost function in (7), a preliminary case study is executed to determine the effect of R_f and L_f on the tracking error of the system. This case study presents the inverter seen in Fig. 1 with L_f = 3mH, R_f =50mΩ and L_g = 0mH (ignoring grid impedance). Then, the system iterates with model values ranging from 50% to 350% of the actual value for both R_f and inductances. The variation of inductance is considered the combined changes in L_g and L_f. By this disturbance metric, when the model values are at 100% of actual parameters, there is no difference between the model and the actual values. Then, the mean square tracking error is recorded for each result. The error is presented as a percentage of the injected RMS current. The surface plot shown in Fig. 2 demonstrates tracking error is lowest near 100% and inductance plays a larger role in tracking error than resistance. Thus, variance in R_f is not considered to reduce the size of the data set and needed complexity of the system.

To collect training data, the conventional MPC without incorporating learned impedance factor is simulated in MATLAB/Simulink at various operating conditions. Table I displays the operating conditions during data collection. The parameters L_g and L_{error} are iteratively changed to account for

changing grid conditions. L_g is varied from 0.5mH to 5mH in 0.1mH increments and L_{error} is varied from 50% to 150% in 1% in increments. L_{error} is the impedance disturbance, the ratio of the actual inductance to the modeled inductance. From these simulations, the 1x8 input array *NNI* at time *k* is extracted as

$$NNI = \begin{bmatrix} err_{(k)}, V_{dc(k)}, V_{pcc(k)}, i_{ref(k)} \\ i_{L(k)}, L_f, V_{pcc(k-1)}, i_{L(k-1)} \end{bmatrix} \quad (9)$$

where *err* is the mean square tracking error, V_{dc} is the dc-link voltage, V_{pcc} is the voltage at the point of common coupling, i_{ref} is the reference current, i_L is the measured inductor current, and L_f is the model inductance. This data collection results in training data set of 2,327,646 samples of the 8 input variables. These are split 70%, 15%, and 15% into training, validation, and testing data respectfully.

The neural network is trained offline using the MATLAB command 'train()'. This creates a shallow feedforward neural network. The constructed network is seen in Fig. 3a and consists of three hidden layers of 8, 25, and 5 neurons respectfully. The output of the neural network is the learned impedance factor ζ as calculated by the disturbance of L_g and L_{error}. To verify the accuracy of the neural network, testing data is used to calculate the error between the actual inductance and the predicted value. The results of this calculation seen in the histogram of Fig. 3b. The testing data show the neural network prediction has ≤ 1% error in 67.9% of test data and ≤ 2% error in 83.4% of test data. This is deemed sufficient for use as the Learned Impedance Factor, and verification of this claim is demonstrated in Section IV.

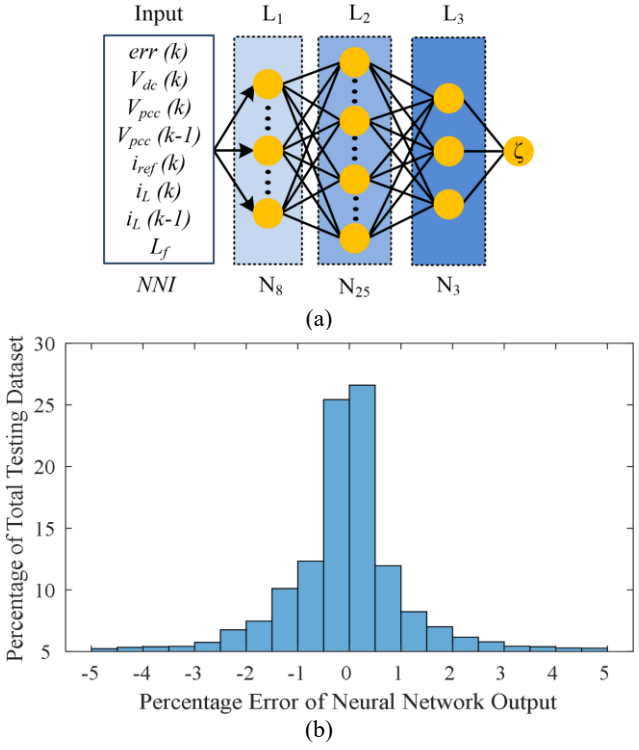

Fig. 3. (a) Diagram of the feedforward neural network used for determining the Learned Impedance Factor. The network input is the vector NNI, utilizes 3 layers of 8, 25, and 3 neurons, and outputs a single variable, ζ. (b) Histogram of the training results of the Neural Network in estimating impedance. The Neural Network can accurately predict the impedance with 2% error of lower in 83.4% of the test data.

IV. Case Study

To verify the operation of the Learned Impedance Factor in MPC, a case study is utilized to examine the proposed control scheme illustrated in Fig. 1. The scenarios are all run using MATLAB/Simulink. In each scenario the MPC is tested with and without the Learned Impedance Factor. When the Learned Impedance Factor is implemented, ζ is actively changing during the converter operation. The input vector *NNI* is feed to the neural network at each sampling instant, which provides the value of ζ at instant *k*. When the Learned Impedance Factor is not implemented, it could be considered that ζ =1.

To examine changing grid conditions, the impedance L_g is varied from 0 to 6 mH in 1 mH increments. In all tests, L_f is equal to 2 mH. All other values match the parameters used for training the neural network, as seen in Table I. In each grid condition, the inverter is run with and without the adaptive ζ implementation, resulting in a total of 14 simulations. In each of these simulations, both the THD and the tracking error are recorded to directly compare the MPC methods. The THD is calculated over 10 cycle periods. The tracking error compares the current injected into the grid to the reference current calculated in (5a) and (5b). To find a single value for tracking error, the total tracking error observed at each instance is combined as a root mean square measurement. This RMS error is then divided by the rated $i_{ref,RMS}$ which for 3 kW is 25 A. This results in a percentage error which is recorded as a single value for each scenario. All data collected through this process are seen in Table II.

An example of this test scenario is seen in Fig. 4. These scenarios demonstrate when L_g is 2 mH. Fig. 4a displays the current waveform which introduces the learn impedance factor at t=0.5s, and Fig. 4b shows the same instance, but illustrates the RMS tracking error. As seen in Fig. 4a the current becomes less distorted and Fig. 4b shows a 78.2% reduction in the tracking error. Additionally, Fig. 5 shows the THD of this same scenario. The THD before the impedance is implemented factor (Fig. 5a) is 3.62% which is reduced to 0.93% after ζ is adaptively implemented factor (Fig. 5b).

As seen in Table II, there is an improvement in the proposed MPC for all L_g values. The largest improvement in THD is at L_g=4 mH, where THD improvement is 2.72% and the largest improvement in tracking error is at L_g = 2 mH where tracking error improvement is 3.51%. This demonstrates improvement for any scenario subject to variable grid impedances. The case studies here only consider impedances up to 6 mH based on the training data range, but these results imply larger impedances could be considered should a larger training data set be utilized in the neural network setup explained in Section III.

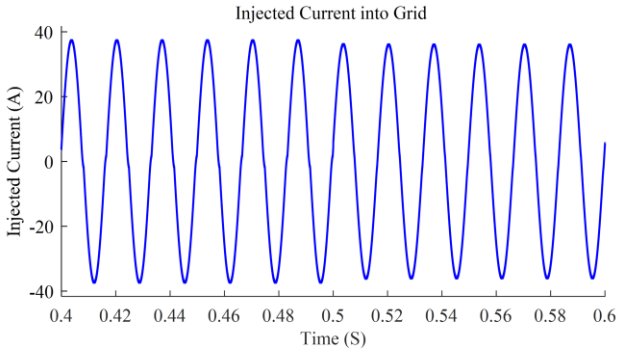

(a)

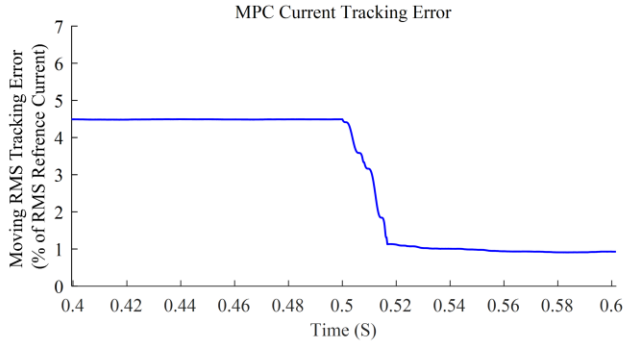

(b)

Fig. 4 Case Study examining the current injected into the grid while comparing a conventional MPC to the MPC utilizing the proposed Learned Impedance Factor. The injected current waveform is seen in (a). Here the Learned Impedance Factor (ζ) is implemented at t=0.5s. The injected current waveform is seen in (a), while the reduction in tracking error is recorded in (b)

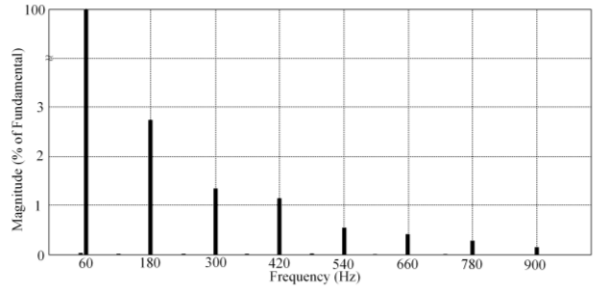

(a)

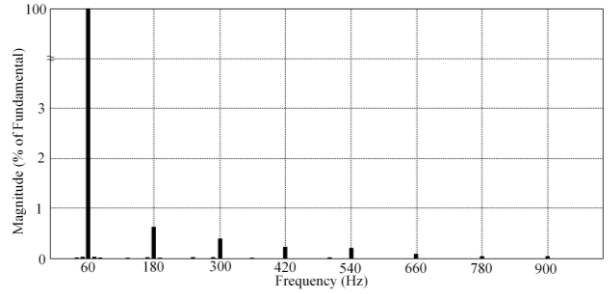

(b)

Fig. 5 The Total Harmonic Distortion of the case study (a) before and (b) after the Learned Impedance Factor is implemented. Total THD is reduced from 3.62% to 0.93%

TABLE. II: CASE STUDY THD AND TRACKING ERROR RESPONSES

	Conventional MPC		MPC with Learned Impedance Factor	
L_g (mH)	THD	Tracking Error	THD	Tracking Error
0	3.56%	4.55%	1.22%	1.40%
1	3.64%	4.56%	1.13%	1.26%
2	3.62%	4.48%	0.93%	0.97%
3	3.53%	4.33%	0.87%	0.87%
4	3.45%	4.13%	0.73%	0.72%
5	3.27%	3.77%	0.67%	0.61%
6	2.97%	3.13%	0.59%	0.50%

TABLE. III: CASE STUDY IMPEDENCE PROFILE

Time	Region	L_g	Learned Impedance Factor
$t < t_1$	I	0 mH	Not Implemented
$t_1 \leq t < t_2$	II	0 mH	Implemented
$t_3 \leq t < t_3$	III	1 mH	Not Implemented
$t_3 \leq t < t_4$	IV	5 mH	Not Implemented
$t_4 \leq t$	V	5 mH	Implemented

The final demonstration of the case study is seen in Fig. 6. This case study demonstrates how the proposed MPC would work in changing grid conditions which could occur in PEDG. This is executed by utilizing the impedance profile seen in Table III. This profile is designed to test both the conventional MPC and the proposed MPC in normal grid conditions (where L_g =0 mH) as well as worsening grid conditions. In Regions II and IV, ζ is adaptively changed according to the neural network, while in the other three regions there is no way of adapting the impedance. L_g is equal to 0 mH for Regions I and II, 1mH for Region III, and 5mH for Regions IV and V. As seen from the waveforms, in all scenarios where the proposed MPC is compared to the conventional MPC the tracking error is reduced once activated. Additionally, there is no penalty to the MPC should the Learned Impedance Factor need to be turned on and off as it is quickly able to adapt to changing greater conditions. This supports the neural network technique, as once the input data is collected from the system it can immediately adapt to the changing grid. From here, it is shown that while operating in its trained region, implementing the proposed MPC will always result in the inverter providing purer current to the grid whether it is experiencing variation in grid impedance or not.

V. CONCLUSION

This paper presents an integrated data-driven and model based predictive control by utilizing neural network for determining disturbances impacting the performance of model predictive controlled grid-interactive inverter. The model used to construct the MPC is detailed, as well as the procedure used to create training data and train the feed forward neural network. This shallow neural network determines the introduced “Learned Impedance Factor” aiming to optimize MPC performance while considering grid condition variation. The learned impedance factor operates with the online MPC to adjust the reference generation signals. This allows the MPC to react to changes in the physical system, allowing the model to

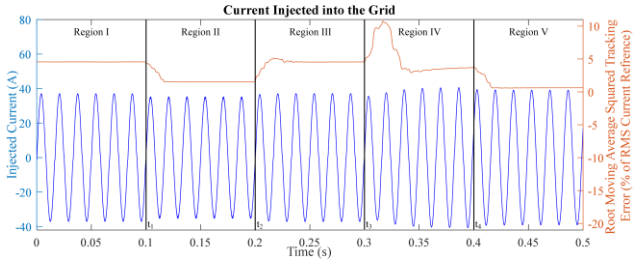

Fig. 6 Examination of how the MPC techniques discussed affect the quality of injected current during changing grid conditions. In this study five operating regions are studied as per the impedance profile seen in Table III. this combines various impedances were and determines whether the learned impedance factor is utilized as seen from the results the scenarios in which the learned impedance factor is utilized always result in a lower tracking error than those in which the impedance is not utilized it also shows no impact to turning on the load impedance factor during operation

remain accurate for effective prediction of control variables. By implementing the learned impedance factor, the grid-tied inverter performance is improved and become more robust to changing grid conditions and other disturbances which would otherwise have negative impacts on the inverter operation, which is expected to occur in PEDG. This is verified through case studies examining the tracking error of the MPC and the total harmonic distortion of the injected grid current. The proposed MPC outperforms the conventional MPC in the considered case study and thus is desirable for implementation in systems with variable grid conditions.

ACKNOWLEDGMENT

This work was supported by the U.S. National Science Foundation under Grant ECCS-2114442. The statements made herein are solely the responsibility of the author.

REFERENCES

[1] S. Kouro, *et al.*, "Model Predictive Control—A Simple and Powerful Method to Control Power Converters," *IEEE Trans. on Ind. Elec.,* vol. 56, no. 6, pp. 1826-1838, 2009.

[2] M. Easley, S. Jain, M. B. Shadmand, and H. Abu-Rub, "Computationally Efficient Distributed Predictive Controller for Cascaded Multilevel Impedance Source Inverter With LVRT Capability," *IEEE Access,* vol. 7, pp. 35731-35742, 2019.

[3] M. Easley, M. B. Shadmand, and H. Abu-Rub, "Hierarchical Model Predictive Control of Grid-Connected Cascaded Multilevel Inverter," *IEEE Journal of Emerging and Selected Topics in Power Electronics,* vol. 9, no. 3, pp. 3137-3149, 2021.

[4] J. Rodriguez *et al.*, "State of the Art of Finite Control Set Model Predictive Control in Power Electronics," *IEEE Transactions on Industrial Informatics,* vol. 9, no. 2, pp. 1003-1016, 2013.

[5] M. Easley, S. Jain, M. Shadmand, and H. Abu-Rub, "Autonomous Model Predictive Controlled Smart Inverter With Proactive Grid Fault Ride-Through Capability," *IEEE Transactions on Energy Conversion,* vol. 35, no. 4, pp. 1825-1836, 2020.

[6] A. Khan, M. Hosseinzadehtaher, M. B. Shadmand, S. Bayhan, and H. Abu-Rub, "On the Stability of the Power Electronics-Dominated Grid: A New Energy Paradigm," *IEEE Industrial Electronics Magazine,* vol. 14, no. 4, pp. 65-78, 2020.

[7] A. Y. Fard and M. B. Shadmand, "Multitimescale Three-Tiered Voltage Control Framework for Dispersed Smart Inverters at the Grid Edge," *IEEE Trans. on Industry Applications,* vol. 57, no. 1, pp. 824-834, 2021.

[8] M. Hosseinzadehtaher, A. Khan, M. Easley, M. B. Shadmand, and P. Fajri, "Self-Healing Predictive Control of Battery System in Naval Power System With Pulsed Power Loads," *IEEE Transactions on Energy Conversion,* vol. 36, no. 2, pp. 1056-1069, 2021.

[9] S. Vazquez *et al.*, "Model Predictive Control: A Review of Its Applications in Power Electronics," *Industrial Electronics Magazine, IEEE,* vol. 8, pp. 16-31, 2014.

[10] E. Garayalde, I. Aizpuru, U. Iraola, I. Sanz, C. Bernal, and E. Oyarbide, "Finite Control Set MPC vs Continuous Control Set MPC Performance Comparison for Synchronous Buck Converter Control in Energy Storage Application," in *International Conference on Clean Electrical Power (ICCEP)*, 2-4 July 2019, pp. 490-495.

[11] M. Easley, M. B. Shadmand, and H. Abu-Rub, "Computationally-Efficient Optimal Control of Cascaded Multilevel Inverters With Power Balance for Energy Storage Systems," *IEEE Transactions on Industrial Electronics,* vol. 68, no. 12, pp. 12285-12295, 2021.

[12] O. H. Abu-Rub, A. Y. Fard, M. F. Umar, M. Hosseinzadehtaher, and M. B. Shadmands, "Towards Intelligent Power Electronics-Dominated Grid via Machine Learning Techniques," *IEEE Power Electronics Magazine,* vol. 8, no. 1, pp. 28-38, 2021.

[13] S. D. silva, M. Shadmand, S. Bayhan, and H. Abu-Rub, "Towards Grid of Microgrids: Seamless Transition between Grid-Connected and Islanded Modes of Operation," *IEEE Open Journal of the Industrial Electronics Society,* vol. 1, pp. 66-81, 2020.

[14] T. Geyer, *Model Predictive Control of High Power Converters and Industrial Drives*. 2016.

[15] S. Vazquez *et al.*, "Model Predictive Control: A Review of Its Applications in Power Electronics," *IEEE Industrial Electronics Magazine,* vol. 8, no. 1, pp. 16-31, 2014.

[16] S. Mariethoz and M. Morari, "Explicit Model-Predictive Control of a PWM Inverter With an LCL Filter," *IEEE Transactions on Industrial Electronics,* vol. 56, no. 2, pp. 389-399, 2009.

[17] Y. Liu, S. Cheng, B. Ning, and Y. Li, "Robust Model Predictive Control With Simplified Repetitive Control for Electrical Machine Drives," *IEEE Transactions on Power Electronics,* vol. 34, no. 5, pp. 4524-4535, 2019.

[18] J. Rodríguez, R. Heydari, Z. Rafiee, H. A. Young, F. Flores-Bahamonde, and M. Shahparasti, "Model-Free Predictive Current Control of a Voltage Source Inverter," *IEEE Access,* vol. 8, pp. 211104-211114, 2020.

[19] M. Easley, A. Y. Fard, F. Fateh, M. B. Shadmand, and H. Abu-Rub, "Auto-tuned Model Parameters in Predictive Control of Power Electronics Converters," in *2019 IEEE Energy Conversion Congress and Exposition*, 29 Sept.-3 Oct. 2019 2019, pp. 3703-3709.

[20] "IEEE Guide for Planning DC Links Terminating at AC Locations Having Low Short-Circuit Capacities," *IEEE Std 1204-1997,* pp. 1-216, 1997.

[21] D. Yang, X. Ruan, and H. Wu, "Impedance shaping of the grid-connected inverter with LCL filter to improve its adaptability to the weak grid condition," *IEEE Transactions on Power Electronics,* vol. 29, no. 11, pp. 5795-5805, 2014.

[22] J. Xu, S. Xie, B. Zhang, and Q. Qian, "Robust Grid Current Control With Impedance-Phase Shaping for LCL-Filtered Inverters in Weak and Distorted Grid," *IEEE Transactions on Power Electronics,* vol. 33, no. 12, pp. 10240-10250, 2018.

[23] C. Bao, X. Ruan, X. Wang, W. Li, D. Pan, and K. Weng, "Step-by-step controller design for LCL-type grid-connected inverter with capacitor–current-feedback active-damping," *IEEE Transactions on Power Electronics,* vol. 29, no. 3, pp. 1239-1253, 2013.

[24] M. F. Umar *et al.*, "Single-Phase Grid-Interactive Inverter with Resonance Suppression based on Adaptive Predictive Control in Weak Grid Condition," *IEEE Journal of Emerging and Selected Topics in Industrial Electronics,* pp. 1-1, 2021.

[25] B. Nun, M. F. Umar, A. Karaki, M. B. Shadmand, S. Bayhan, and H. Abu-Rub, "Rank-based Predictive Control for Community Microgrids with Dynamic Topology and Multiple Points of Common Coupling," *IEEE Journal of Emerging and Selected Topics in Industrial Electronics,* pp. 1-1, 2021.

[26] A. J. Agbemuko, J. L. Domínguez-García, O. Gomis-Bellmunt, and L. Harnefors, "Passivity-Based Analysis and Performance Enhancement of a Vector Controlled VSC Connected to a Weak AC Grid," *IEEE Transactions on Power Delivery,* vol. 36, no. 1, pp. 156-167, 2021.